

Load Forecasting for Households and Energy Communities: Are Deep Learning Models Worth the Effort?

Lukas Moosbrugger ^{a,*}, Valentin Seiler ^a, Philipp Wohlgenannt ^a,
Sebastian Hegenbart ^b, Sashko Ristov ^c, Peter Kepplinger ^a

^a*illwerke vkw Endowed Professorship for Energy Efficiency, Energy Research Centre, Vorarlberg University of Applied Sciences, Dornbirn, Austria*

^b*Digital Factory Vorarlberg GmbH, Dornbirn, Austria*

^c*Department of Computer Science, University of Innsbruck, Innsbruck, Austria*

Abstract

Accurate load forecasting is crucial for predictive control in many energy domain applications, with significant economic and ecological implications. To address these implications, this study provides an extensive benchmark of state-of-the-art deep learning models for short-term load forecasting in energy communities. Namely, LSTM, xLSTM, and Transformers are compared with benchmarks such as KNNs, synthetic load models, and persistence forecasting models. This comparison considers different scales of aggregation (e.g., number of household loads) and varying training data availability (e.g., training data time spans). Further, the impact of transfer learning from synthetic (standard) load profiles and the deep learning model size (i.e., parameter count) is investigated in terms of forecasting error. Implementations are publicly available and other researchers are encouraged to benchmark models using this framework. Additionally, a comprehensive case study, comprising an energy community of 50 households and a battery storage demonstrates the beneficial financial implications of accurate predictions. Key findings of this research include: (1) Simple persistence benchmarks outperform deep learning models for short-term load forecasting when the available training data is limited to six months or less; (2) Pretraining with publicly available synthetic load profiles improves the normalized Mean Absolute Error

*Corresponding author. Email: lukas.moosbrugger@fhv.at

(nMAE) by an average of 1.28%pt during the first nine months of training data; (3) Increased aggregation significantly enhances the performance of deep learning models relative to persistence benchmarks; (4) Improved load forecasting, with an nMAE reduction of 1.1%pt, translates to an economic benefit of approximately 600€ per year in an energy community comprising 50 households.

Keywords: Load Forecasting, Deep Learning, Transformer, xLSTM, Transfer Learning, Energy Communities

1. Introduction

For the management of energy assets, model predictive control (MPC) methods are used with great success^{1,2}. In practice, MPC relies on accurate forecasts for exogenous variables such as load, production, or emissions. Thus, forecasting short-term load is a crucial part for the optimized operation of flexible energy assets³.

Increasingly popular entities, concerned with the control of flexible assets, are Energy Communities (ECs). ECs are groups of individuals or organizations that produce, manage, and consume energy locally, through the use of public grid infrastructure, often with the goal of increasing sustainability and reducing energy costs⁴. Efficient control of their energy assets through, for example, MPC can increase their financial benefit⁵.

Even though this works' focus is on ECs, aggregated household load forecasting can be applied in other applications as well. While small ECs are similar to the load behaviors of individual households, larger ECs are similar to the load profiles of secondary substations. Numerous models have already been proposed for short-term load forecasting, covering time horizons ranging from one hour up to one week³. In recent years, neural networks using Long Short-Term Memory (LSTM) have been widely regarded as popular models for short-term load forecasting of households^{3,6,7}. However, more recently, many studies have replaced LSTMs with Transformer models due to their ability to handle long-range dependencies and efficiently parallelize computations. For example, Semmelmann et al.⁸ compared the forecasting errors of LSTMs and Transformers for an EC consisting of 21 households and concluded that Transformer models outperformed LSTMs. Similarly, Ran et al.⁹ achieved the same result when evaluating a single highly aggregated load profile representing the entire city of New York. Likewise, Zhao et al.¹⁰

found that Transformers significantly outperformed LSTMs, using data from a single aggregated load profile representing New South Wales, Australia. L’Heureux et al.¹¹ showed that a Transformer-based model outperformed a state-of-the-art recurrent model when tested on 20 highly aggregated load profiles from an energy utility company. Fang et al.¹² also reported similar findings, where a Transformer-based approach surpassed an LSTM-based model using a single high-aggregation load profile from one zone of Tetouan city.

In May 2024, Beck et al.¹³ introduced the xLSTM model. The authors claimed that this model performs favorably when compared to state-of-the-art Transformers, both in performance and scaling. They demonstrated that xLSTM exhibits performance comparable to Transformers, with notable advantages such as linear rather than quadratic growth in memory consumption as the model input size increases. This improvement addresses scalability challenges, making xLSTM a more efficient option to handle larger inputs. A first work by Kraus et al.¹⁴ demonstrates the effectiveness of xLSTM for long-term forecasting across various publicly available time series, with forecast horizons ranging from 96 to 720 hours, in contrast to the short-term forecasting problem addressed in this study.

One practical problem of such deep learning models in ECs is that they often lack enough historical data¹⁵. This potentially leads to poor system performance. Transfer learning is a promising approach to overcome this problem. This approach is based on the idea that knowledge learned during one task can be reused to boost the performance on a related task¹⁶. In Moosbrugger et al.¹⁷, the potential of leveraging transfer learning was demonstrated using open-access synthetic (also called *standard*) load profiles to improve load forecast error for renewable ECs with limited historical data. The study utilized a bidirectional LSTM model pre-trained on open-access synthetic profiles, achieving a notable reduction in mean squared error (MSE) from 0.34 to 0.13 in a test EC involving 74 households. Furthermore, this approach significantly improved training stability.

Compared to the load forecasting studies mentioned, this research is broader in scope. Profiles, aggregation levels, training data durations, seasons, and model sizes are varied, providing a more comprehensive evaluation. This approach aligns with the recommendation of Pinheiro et al.¹⁸, who noted that many existing studies demonstrate the superiority of a proposed technique on narrowly defined datasets, often hiding their weaknesses. By introducing diverse setups, this study seeks to reflect realistic variations,

providing insights that are both more generalizable and practically applicable. In addition, a case study is presented that quantifies the financial implications of different forecast errors. In the case study, MPC is applied to a simulated EC with different forecasting algorithms.

In summary, the key contributions of this paper are as follows:

1. The performance of state-of-the-art deep learning models in short-term load forecasting is evaluated, with the recently proposed xLSTM model compared against established approaches such as LSTM and Transformers.
2. The forecast error is investigated based on the aggregation level of ECs and different training data sizes.
3. The effectiveness of different prediction methods during different stages considering data availability is investigated thoroughly.
4. The financial benefits of improved forecast errors are illustrated through a case study.

2. Methods

To assess the performance of all models for the various given use cases, a software framework is designed and implemented, detailed in this Section. Specifically, three deep learning models - xLSTM, LSTM, and Transformer - are compared against three basic models: Persistence Prediction, k-Nearest Neighbors (KNN), and forecasting with synthetic load. Each model performs day-ahead short-term load forecasting, generating 24 hourly load predictions spanning from midnight to midnight. The xLSTM, LSTM, Transformer, and KNN models utilize standard input features for short-term load forecasting, including datetime information, weather conditions, and historical load data, as utilized by Pinheiro et al.¹⁸.

The models are trained and tested on various configurations of ECs, aggregation sizes, training dataset sizes, seasons, and model parameter counts. A parameter grid is constructed, and a baseline setup is defined. This baseline allows to systematically analyze how forecast errors vary when specific parameters are individually adjusted. This enables to manage the complexity of the analysis while maintaining a focus on the most critical factors influencing model performance. More documentation, the full implementation, and the datasets used can be found in the corresponding GitHub repository¹⁹.

2.1. Use Cases

Each of the following subsections explains one dimension of the parameter grid constructed for analysis. The use cases are designed to ensure both practicality and relevance, with key aspects outlined below.

2.1.1. Aggregation Size

To investigate different levels of aggregation, five different community sizes have been selected for comparison. The Austrian Coordination Office for Energy Communities²⁰ categorizes most ECs in Austria into 2–10, 10–50, or 50–100 households. Based on this classification, the boundary cases of 1, 2, 10, 50, and 100 households are selected for analysis. In the parameter grid, 50 households are chosen as the baseline aggregation size, representing a central point between 1 and 100. This baseline serves as a reference point for systematically evaluating the forecast error.

2.1.2. Training Size

To evaluate the practical challenge of insufficient training data, varying training dataset sizes are considered. The evaluation starts with as little as 2 months of training data, progressively increasing to 4, 6, and 9 months. A reasonable training size is 12 months, as this ensures that the model has been exposed to all seasons of the year, providing a robust baseline. Furthermore, 15 months are included, representing the maximum training size available in the dataset used, as described in Section 3.5.

2.1.3. Date of the Test Set

In practice, time series forecasting relies on historical training data to forecast future time horizons. Using future data could be considered impractical or data leakage, as future knowledge might be leaked to the past. Following this, the final quarter of 2013 is assigned as the baseline test set, while the directly preceding months form the training set.

In order to ensure that this chosen test set is reasonable and balanced, the following preliminary analysis is conducted. Due to the limited amount of available data (as explained in Section 2.2), it is not feasible to maintain 12 months of training data prior to each potential test date throughout the year. To address this, the year 2013 is divided into four quarters, with each quarter sequentially used as the test set while the remaining three quarters form the training set. This cross-validation strategy maximizes the utility of the dataset and provided a robust framework for evaluating model performance

across the entire year. The results of this experiment (presented in Section 9) validate the final choice of quartal Q4 2013 as the test set.

2.2. Dataset

The dataset used in this study is derived from the smart meter energy consumption data provided by the UK Power Networks⁷, which includes records from 5,567 households in London. To construct virtual ECs, subsets of 2, 10, 50, or 100 households were randomly selected from the refined dataset. This selection process was repeated 20 times for each category of community size, without replacement, resulting in $20 \cdot 4 = 80$ unique virtual ECs, along with 20 individual household profiles. All profiles span the period from July 2012 to February 2014, providing a robust foundation for the analysis.

Additionally, synthetic load profiles were used, as it will be described in Section 2.3. For these purposes, the German synthetic load profiles provided by the Python package *demandlib* were employed. This package generates hourly synthetic load data for an arbitrary year and can even forecast loads for future years, making it a useful resource for transfer learning applications.

2.3. Models

This section describes the deep learning models used (xLSTM, LSTM, and Transformer) and the basic models (Persistence Prediction, KNN, and Forecasting with Synthetic Load). It is important to note that a separate model is trained for each distinct EC.

2.3.1. Basic Models (Non Deep Learning)

The aforementioned state-of-the-art deep learning models are benchmarked against three simple and commonly used methods:

Persistent Prediction Model: This benchmark model predicts the next day to be exactly the same as it was 7 days ago. Gross et al.²¹ call this also the naive seasonal model.

KNN²¹: This model utilizes the same input features as the deep learning models, described in 2.3.3. In the implementation of this study, k was set to 1, meaning the model predicts the next day based on the day with the most similar features according to Euclidean distance.

Synthetic Load Profile Predictor: This method sets the next day’s load profile equal to the synthetic (standard) load profile for the next day.

2.3.2. Deep Learning Models

Two very popular deep learning methods for load forecasting are selected from the literature review^{3,6,7,8,9,10,11,12} for this comparative study : LSTMs and Transformers. Additionally, a new model, xLSTM¹³, is chosen.

The general model architecture used in this study is illustrated in Fig. 1. Similar to many established LSTM-based applications (see, e.g., Kong et al.⁶), the LSTM layer is followed by multiple dense (i.e., feedforward neural network) layers. We use the same approach for xLSTMs. For the Transformer model, an encoder-only architecture is adopted, as demonstrated by Nie et al.²². To ensure fair comparability across the different sequence-to-sequence deep learning models, the dense layers at the output are designed with a fixed number of neurons.

Each model was constructed with a varying number of parameters, targeting a count of 1k, 2k, 5k, 10k, 20k, 40k, and 80k. This spans a further dimension of the parameter grid of this study, as will be explained in Section 2.3.4. Model details are summarized in Appendix A. Please note that the parameter counts of the models do not match exactly due to their nature of computation, but were selected to be as close as possible.

All models are trained with Adam²³ optimizer over 100 epochs, with dynamic learning rate from 0.01 to 0.0005 and using batch sizes of 256.

2.3.3. Deep Learning Input Features

The current datetime, past weather data, and past load values are used as input features, which are, for instance, also used by Pinheiro et al.¹⁸. These hourly model input features are detailed as follows:

- Inputs 0-6: The day of week is encoded as a one-hot vector, represented as a binary 7-dimensional vector with one "hot" bit. Public holidays are mapped to Sundays.
- Inputs 7-8: Hour of day, encoded cyclically. The hour of day is mapped onto a unit circle using sine and cosine transformations to preserve its cyclical nature.
- Inputs 9-10: Day of year, encoded cyclically, similar to the hour of day feature.
- Inputs 11-13: Lagged load profiles. These features include the hourly load measurements from exactly 1, 2, and 3 weeks prior to the current timestep.

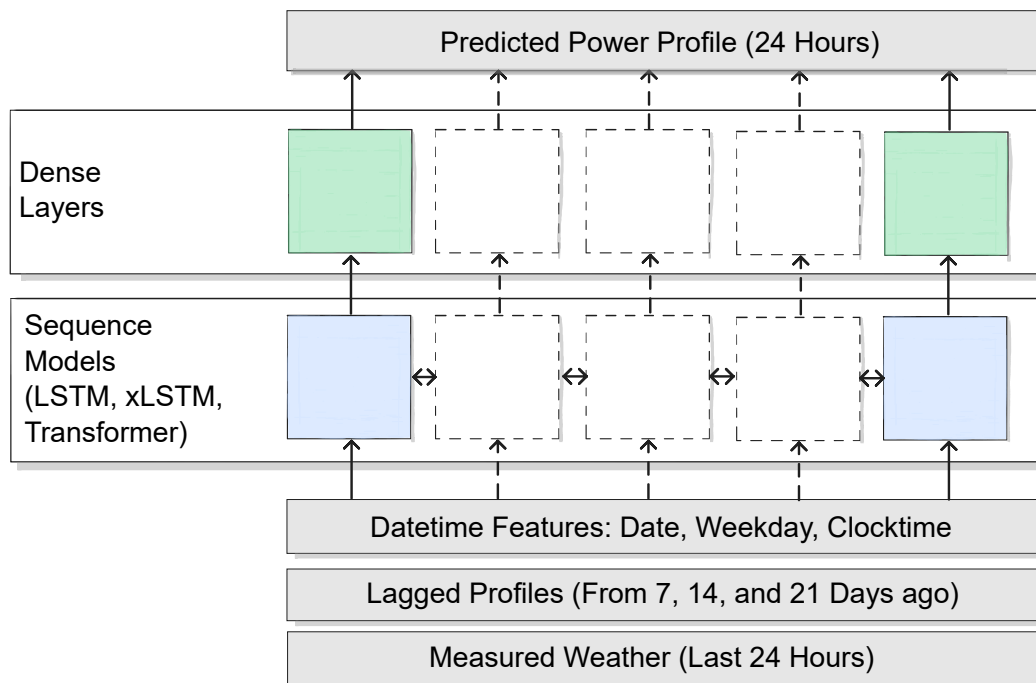


Figure 1: The sequence-to-sequence deep learning models used in this study. The lower square blocks represent xLSTM cells, bidirectional LSTM cells, or Transformer Encoder layers, while the upper square blocks represent dense layers. To enable a fair comparison among the models, the number of parameters for each model was varied to fall within a comparable range.

- Inputs 14-19: Weather data. All available Meteostat²⁴ weather features for London from 2011 to 2014 are utilized. These features include temperature, dew point, wind direction, wind speed, air pressure, and relative humidity from the last 24 hours before the forecast.

2.3.4. Model Size

When tuning hyperparameters of these deep learning models, the aim is to ensure that the model sizes (measured by parameter count) are roughly comparable across architectures. Similar to the test set selection process described in Section 2.1.3, preliminary analyses are conducted to identify effective model sizes. The results of these experiments (presented in Section 3.3) indicate that a target model size of 5k parameters serves as a good baseline. This size achieved robust performance across all models and lies at the midpoint of the parameter range, balancing model complexity and forecast error.

2.3.5. Transfer Learning

Building on the authors’ previous work¹⁷, transfer learning is applied using synthetic load profiles. During pretraining, models are exposed to synthetic load profiles spanning the entire period from July 2012 to February 2014. The learned parameters from this phase are saved and later loaded before fine-tuning the model with real EC profiles. The results were generated with and without transfer learning. The baseline for the parameter grid includes transfer learning.

2.4. Implementation and Evaluation

The models are trained using the Mean Absolute Error (MAE) loss, as energy applications typically prioritize minimizing absolute errors rather than squared errors, due to the linear relation between energy costs and used energy:

$$\text{MAE} = \frac{1}{n} \sum_{i=1}^n |y_i - \hat{y}_i| \quad (1)$$

To enable comparisons across ECs of varying sizes within the same table or figure, the results are evaluated using the normalized Mean Absolute Error (nMAE):

$$\text{nMAE} = \frac{\text{MAE}}{\bar{y}} \quad (2)$$

where the normalization factor \bar{y} represents the mean of all n values.

The framework is evaluated on an Ubuntu 22.04 system. To ensure reproducibility, a conda environment file is supplied, detailing the primary dependencies, including Python 3.11²⁵ and PyTorch 2.2²⁶.

The experiments are designed to evaluate the impact of various factors on the forecast error, including model size, time of year, community size, and training set size. The baseline configuration, as explained in the individual sections above, is defined with the following parameters: A model size of 5k parameters, a test set corresponding to Q4 2013, a community size of 50 households, and a training set spanning 12 months. From this baseline, a systematic exploration is conducted to examine how the forecast errors varied when individual parameters were adjusted.

3. Results and Discussion

This chapter provides insights into the performance of state-of-the-art forecasting models across various ECs and aggregation levels. As previously described, all experiments are conducted using the baseline configuration (i.e., a model size of 5k parameters, a test set corresponding to the fourth quarter (Q4), a community size of 50 households, and a training set spanning 12 months). Starting from this baseline, a systematic exploration examines how forecast errors vary with adjustments to individual parameters. Key findings are presented in this section, whereas detailed numerical results, including comprehensive data for all models, are provided in Appendix B. Please note that the KNN and Synthetic Load Profile models exhibited significantly higher errors compared to other approaches. While these models are excluded from the following figures for clarity, their results are fully documented in Table B.3 and Table B.4 for reference.

3.1. Forecast for One Sample Energy Community

The results of Fig. 2 showcase the daily forecasts for a sample EC using the baseline configuration. This figure demonstrates that the forecast error is low for the largest part of the test set. In particular, the daily nMAE for Monday through Saturday during October and November remains consistently stable at around 10% for most days. An example of a day with strong

forecast accuracy is illustrated in Fig. 3b. As expected, forecast errors peak during the Christmas holidays, reflecting the distinct energy consumption patterns of the holiday season. This anomaly is illustrated in Fig. 3a.

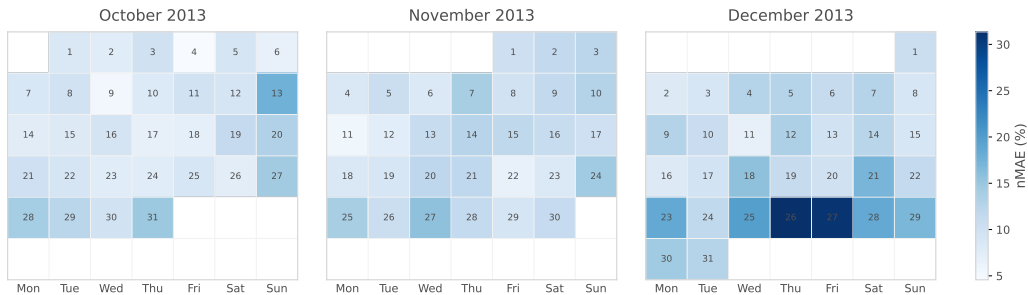


Figure 2: Daily forecast error for a randomly sampled EC using the Transformer model with the baseline configuration (model size of 5k parameters, a test set corresponding to Q4 2013, a community size of 50 households, and a training set spanning 12 months).

3.2. Training with Limited Data

Fig. 4 illustrates the performance improvement of the deep learning models over growing training data compared to the persistence prediction benchmark. Notably, the mean forecast error of the persistence predictor outperforms that of the deep learning models with up to six months of training data. However, with 9 months of training data, the deep learning models outperform persistent prediction, with a mean improvement ranging from 0.65%pt to 1.53%pt, depending on the model type. This finding is particularly valuable for newly established ECs, which can initially rely on persistence prediction and transition to deep learning models at 9 months.

Fig. 4 further demonstrates that the forecast error decreases significantly as the size of the training data increases. The models demonstrate improved generalization to new days when trained on a larger volume of historical data. However, this reduction in error appears to plateau at approximately 12 months of training data, indicating diminishing returns from additional historical data beyond this point. This suggests that the model effectively captures all seasonal patterns within that training period.

Finally, as illustrated in Fig. 5, transfer learning using synthetic load profiles shows a notable reduction in mean forecast errors for small training sizes. Across all models, the average improvement for training durations of 2, 4, and 6 months is 1.28%pt. Remarkably, this improvement is achieved despite

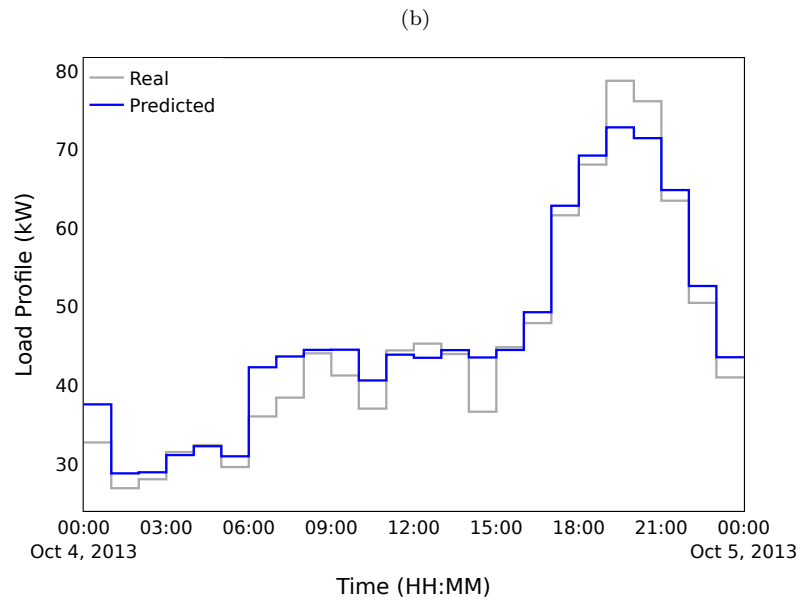
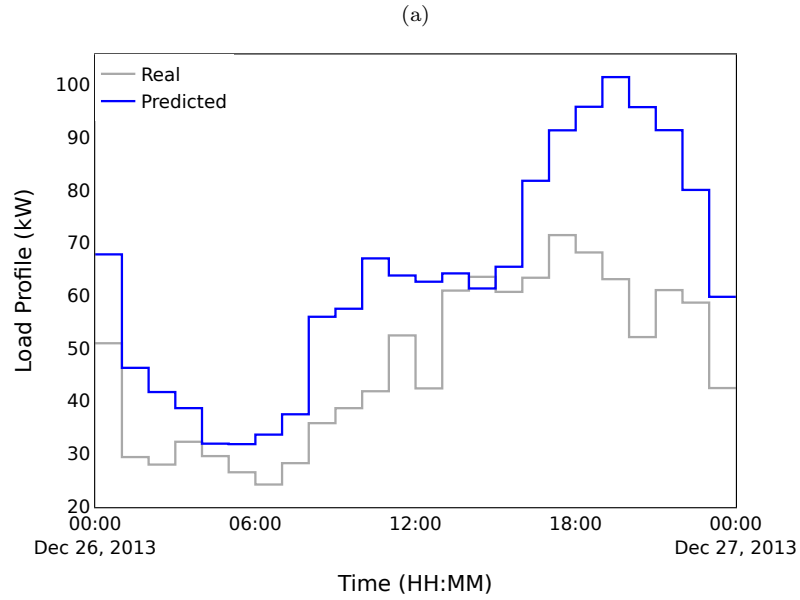


Figure 3: Load Forecasts of a randomly sampled EC using the Transformer model with the baseline configuration (model size of 5k parameters, a test set corresponding to Q4 2013, a community size of 50 households, and a training set spanning 12 months). (a) shows a day with poor accuracy ($nMAE = 20.7\%$). Here especially the evening peak is clearly underestimated. (b) depicts a day with decent accuracy ($nMAE = 6.5\%$).

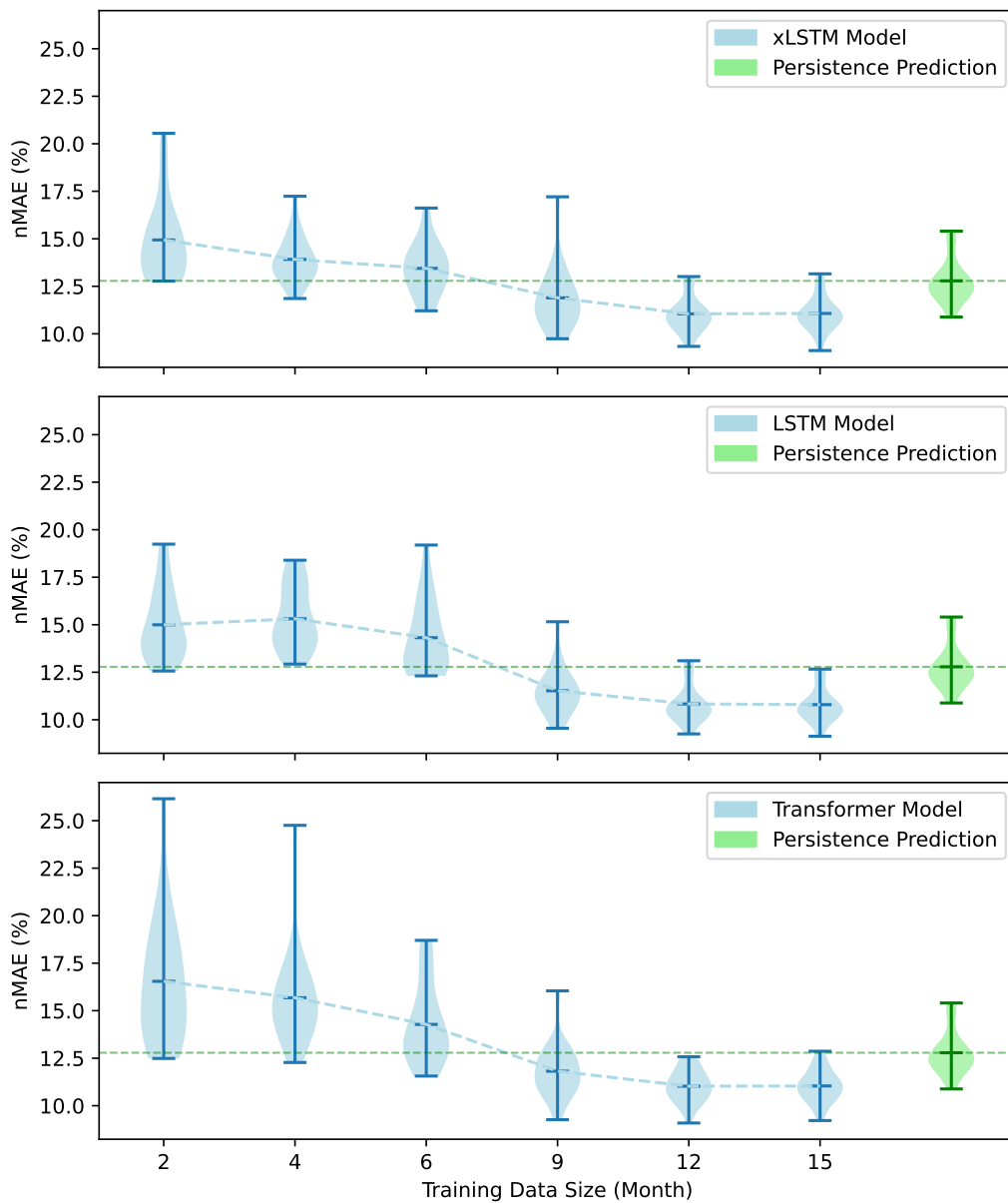


Figure 4: Load forecasting with different training data sizes. Each setting includes results from 20 randomly sampled ECs, based on the baseline configuration (model size of 5k parameters, a test set corresponding to Q4 2013, and a community size of 50 households).

using synthetic profiles from Germany rather than the UK for pretraining. Only with a training duration of 9 months or longer the mean improvement approaches zero, as the model has already been exposed to most seasons of the year. This finding underscores the versatility and generalizability of synthetic profiles as a robust pretraining dataset, particularly for cases with limited training data. Unlike specific profiles that may risk overfitting the models, synthetic profiles demonstrate broad applicability across diverse scenarios.

3.3. Impact of the Model Size

Fig. 6 illustrates the relationship between model size and forecast error. The results reveal several noteworthy insights. One observation is that the Transformer model demonstrated highly stable performance across varying model sizes, i.e., across different hyperparameter settings. The mean nMAE fluctuates by at most 0.35%pt, while also the standard deviation remained nearly independent of the model’s parameter count, with a maximum fluctuation of 0.19%pt. This plot also reveals that larger sequence models do not necessarily produce better results, which may be contrary to common expectations. In contrast, the models can be configured with as few as 2k or fewer parameters, yet still deliver low forecast errors. This finding is especially relevant for small edge computing devices, such as home automation systems with limited computational resources, as it suggests that smaller, more efficient models can achieve comparable performance without the need for extensive computational power.

3.4. Impact of Different Community Sizes

Fig. 7 illustrates the relationship between the forecast error and the size of the EC. As anticipated, the forecast error decreases substantially with increasing community size. At the same time, as the size of the community increases, the forecast deviation gets significantly smaller. This trend, illustrated here using the Transformer architecture, is consistently observed across all models in the study. Fig. 8 shows that at all aggregation levels, the mean performance of the persistence predictor is consistently worse than that of deep learning models. This effect becomes particularly pronounced at a higher aggregation size of e.g. 100 households, where the forecast deviation is comparably small.

Finally, it is worth emphasizing that all three deep learning models exhibit comparable performance across various community sizes, with only mi-

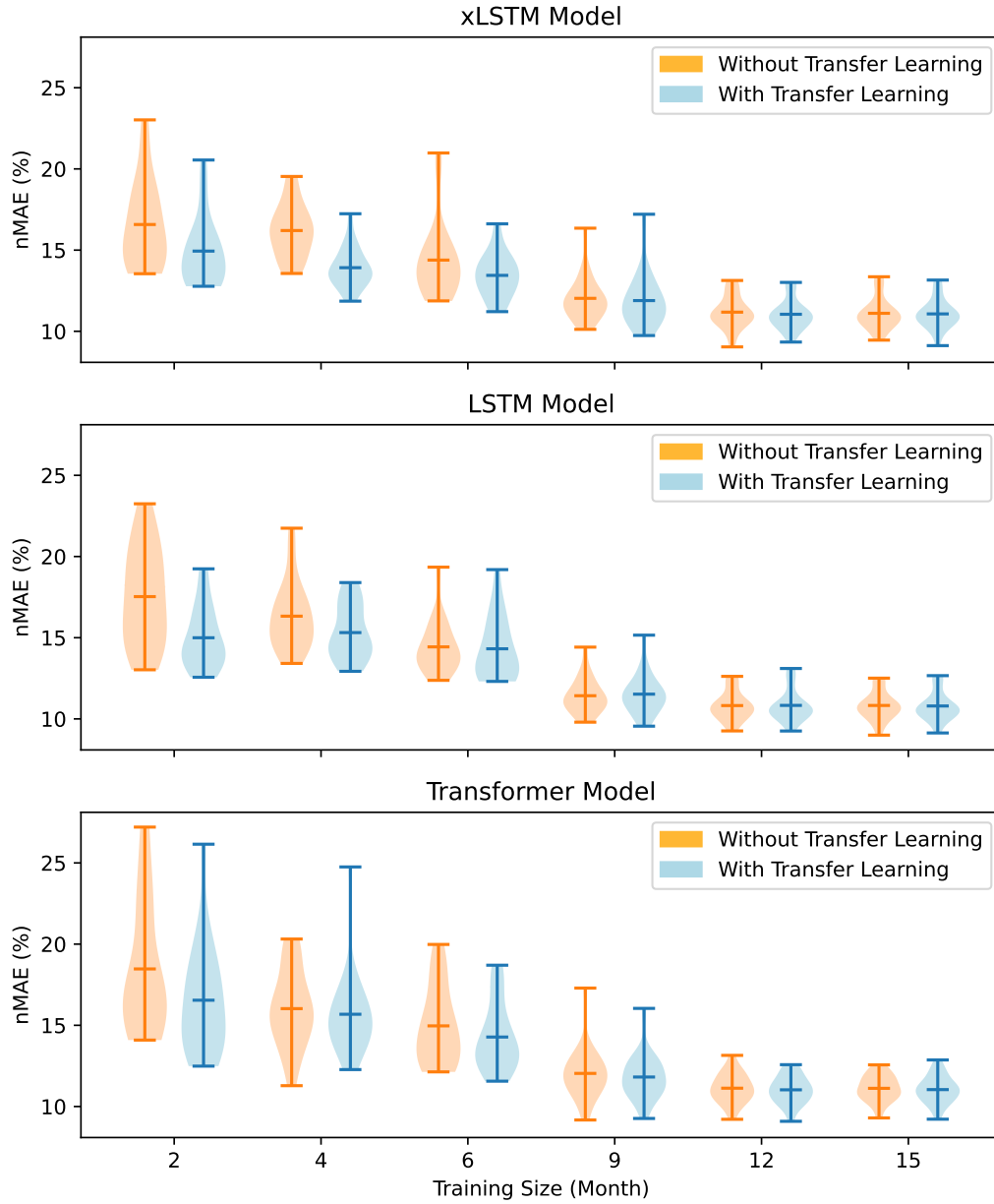


Figure 5: Effect of transfer learning over the training size. Each setting includes results from 20 randomly sampled ECs, based on the baseline configuration (model size of 5k parameters, a test set corresponding to Q4 2013, and a community size of 50 households).

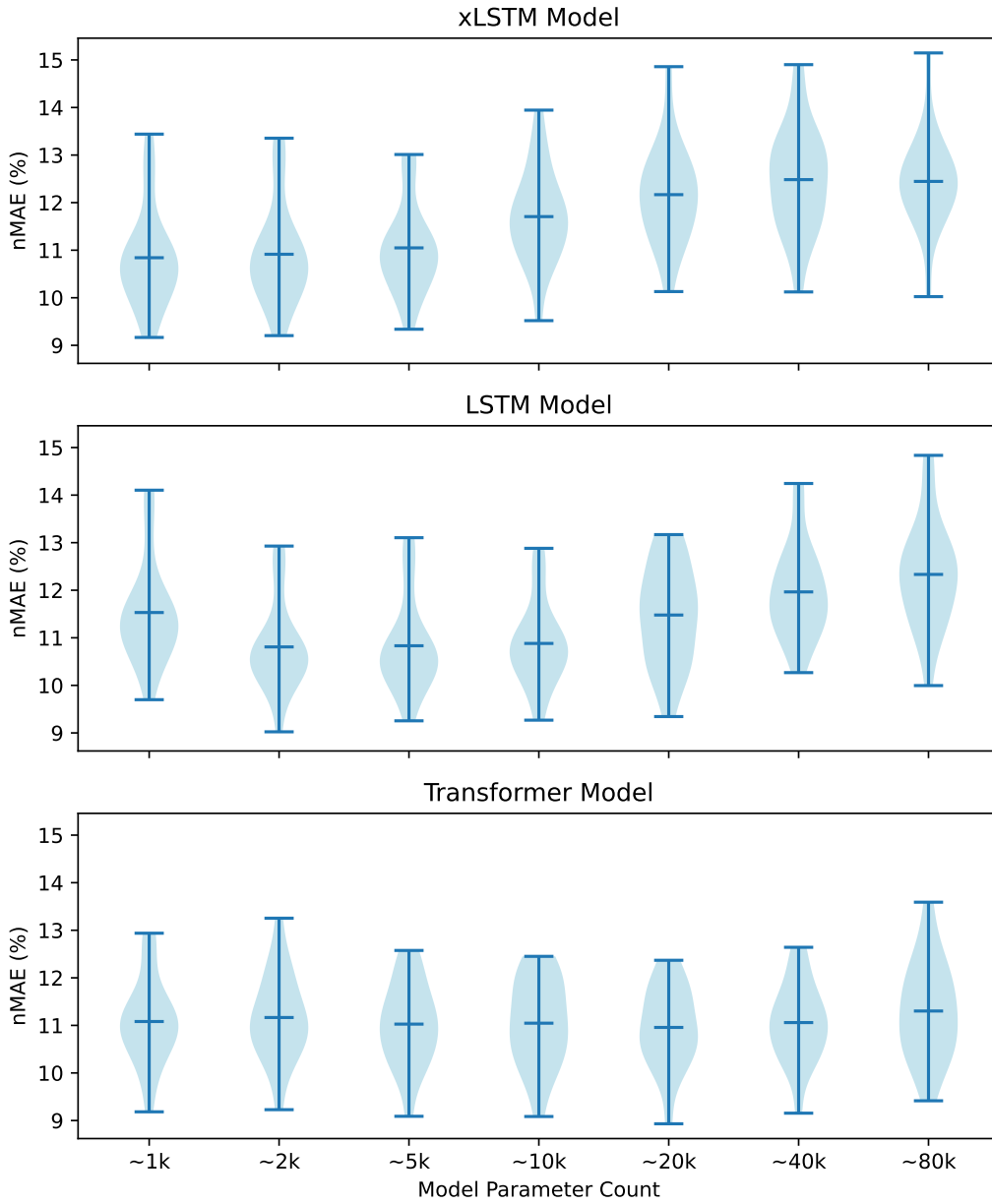


Figure 6: Load forecasting error as a function of model parameter count. Each setting contains results from 20 randomly sampled ECs using the baseline configuration (a test set corresponding to Q4 2013, a community size of 50 households, and a training set spanning 12 months).

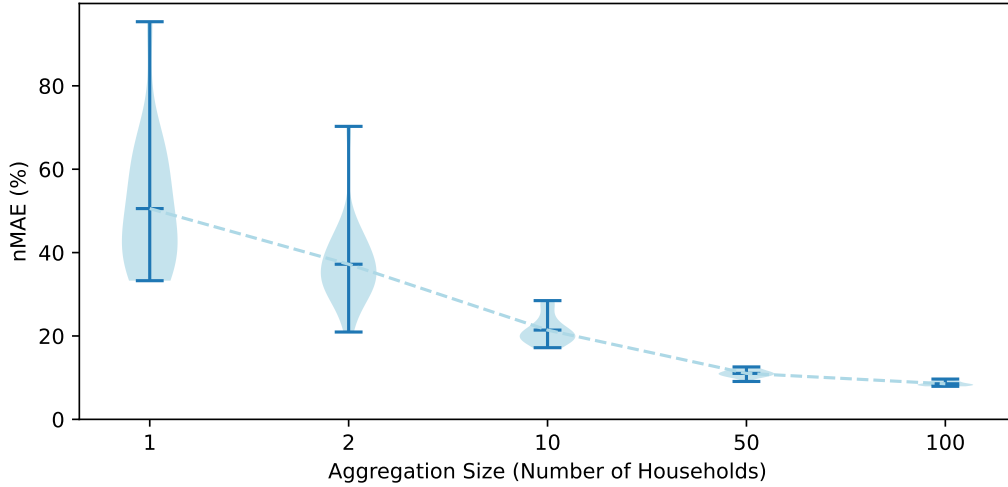


Figure 7: Load forecasting error across different aggregation sizes, illustrated using the Transformer model. Each setting contains results from 20 randomly sampled ECs using the baseline configuration (model size of 5k parameters, a test set corresponding to Q4 2013, and a training set spanning 12 months).

nor differences observed. As a result, any of these models can be selected for load forecasting. The model choice can therefore be based on specific needs or preferences, without concerns about significant variations in forecast error. This enables users to prioritize factors such as ease of implementation, computational efficiency, or seamless integration with existing systems.

3.5. Impact of the Testing Quarter of the Year

Based on the train-test-split methodology discussed in Section 2.1.3, Fig. 9 presents the error of the test set in the different quarters of 2013. The results demonstrate that the load forecasting models employed in this study perform consistently well throughout the entire year. All quarters show consistently results with similar error ranges, confirming that Q4 2013 serves as a representative and balanced benchmark for evaluation.

4. Case Study

This section presents a simulation case study to quantify the financial implications of forecasting errors within an EC. The objective is to reduce daily energy costs via intraday load shift. The EC consists of 50 households

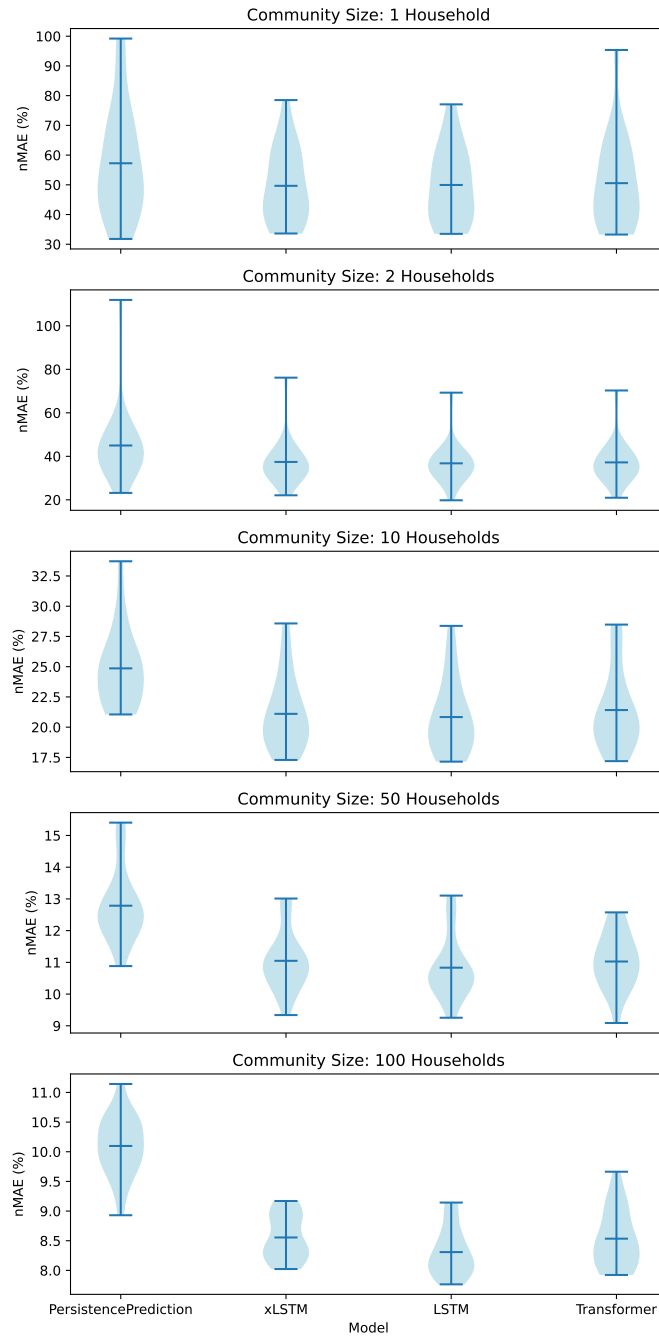


Figure 8: Load forecasting over different aggregation sizes. Each setting contains results from 20 randomly sampled ECs using the baseline configuration (model size of 5k parameters, a test set corresponding to Q4 2013, and a training set spanning 12 months).

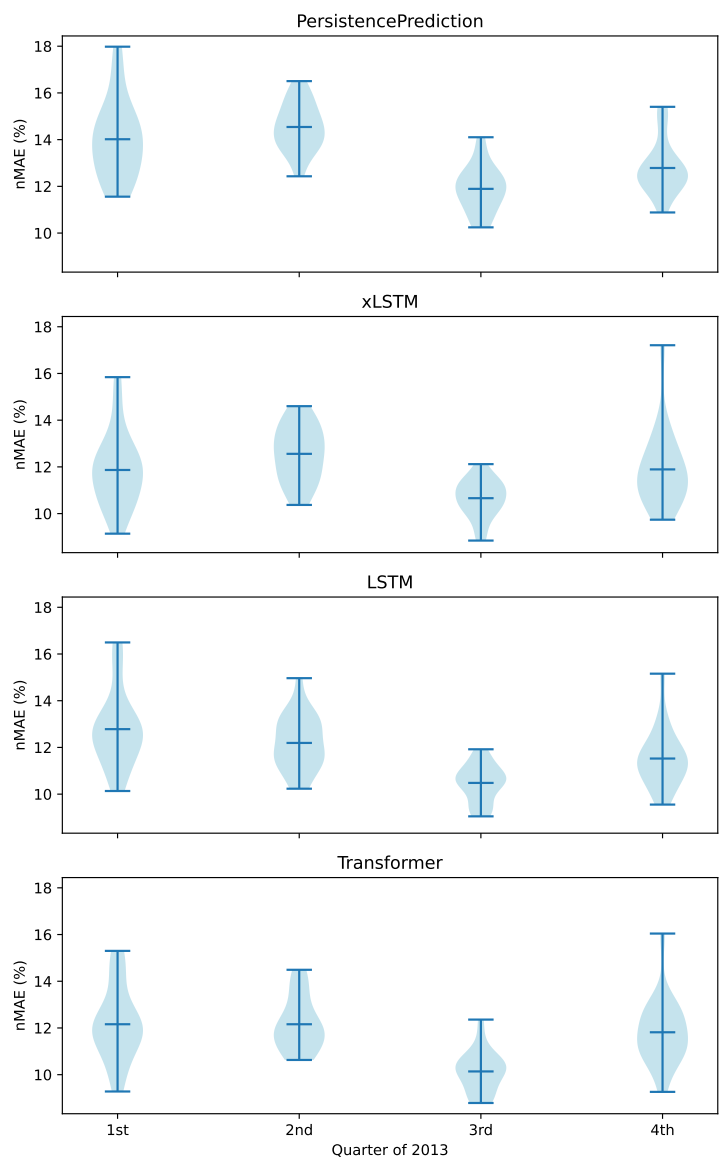


Figure 9: Load forecasting across the quarters of the year 2013. Each setting was tested against 20 randomly sampled ECs using the baseline configuration (model size of 5k parameters, a community size of 50 households, and a training set spanning 12 months).

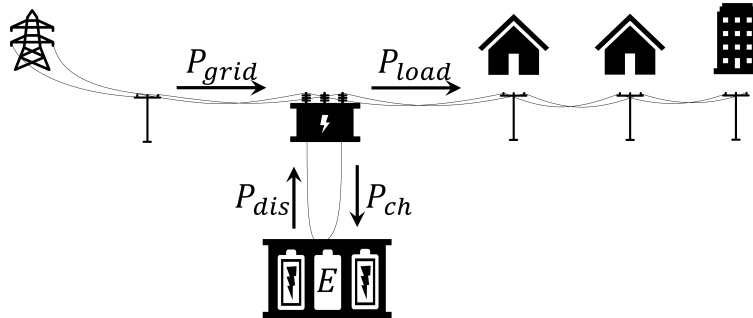


Figure 10: Scheme of the case study EC with community battery energy storage system.

and a community battery energy storage system (BESS) assumed to be located in Austria. It has a real-time price (RTP) tariff based on the European Power Exchange (EPEX)²⁷. In this case study, the Energy Exchange Austria (EXAA)²⁸ is used in combination with network usage fees and taxes according to current Austrian standards. A 4-hour (C-Rate = 0.25) BESS with a capacity of 1 MWh with a round-trip efficiency of 85%²⁹ is installed. The BESS is used for load shifting, to minimize the EC electricity costs. The simulation is executed for the test period from 1st October 2013 to 31st December 2013 and the simulation is discretized to hourly time steps Δt .

Fig. 10 shows a systematic overview of the simulation case study. Here, E is the energy stored in the BESS, P_{ch} is the charging power, P_{dis} is the discharging power, P_{load} is the electrical load of the EC and P_{grid} is the power consumption from the grid, which has to be purchased.

The BESS is controlled to minimize the EC cost by applying load shifting e.g. to shift the load from high price periods to low price periods during one day. Load shifting is optimized once a day via Mixed Integer Linear Programming (MILP). Therefore, energy prices and loads are needed. Future day ahead energy prices ($\hat{\pi}_p$) are available from the day ahead stock exchange such as EPEX and EXAA. Thus, a perfect prediction for energy prices is a realistic scenario and can be assumed. However, for future loads (\hat{P}_{load}), a forecast is required.

The optimization model distinguishes between state variables and process variables. State variables are indexed via t and defined for one time point, while process variables are indexed via p and defined for one time period. N periods result in $N + 1$ time points. E_t is the state variable and $P_{ch,p}$, $P_{dis,p}$, $\hat{P}_{load,p}$, $\hat{P}_{grid,p}$ and $\hat{\pi}_p$ are the process variables. The MILP uses the forecasted

load profile $\hat{P}_{\text{load},p}$ and the RTP $\hat{\pi}_p$ as inputs. Note, that the hat symbol $\hat{\cdot}$ denotes the forecasted/uncertain variables. The resulting optimization problem for one day can be written as:

$$\min_{P_{\text{ch}}, P_{\text{dis}}} \sum_{p \in \mathcal{P}} \hat{P}_{\text{grid},p} \hat{\pi}_p \Delta t \quad (3)$$

$$\mathcal{P} = \{0, \dots, 23\} \quad (4)$$

$$\mathcal{T} = \{0, \dots, 24\} \quad (5)$$

s.t. $\forall p \in \mathcal{P}$:

$$\hat{P}_{\text{grid},p} + P_{\text{dis},p} = P_{\text{ch},p} + \hat{P}_{\text{load},p} \quad (6)$$

$$E_{p+1} - E_p = (\eta_{\text{ch}} P_{\text{ch},p} - \frac{P_{\text{dis},p}}{\eta_{\text{dis}}}) \Delta t \quad (7)$$

$$0 \leq P_{\text{ch},p} \leq b_{\text{ch},p} P_{\text{BESS,max}} \quad (8)$$

$$0 \leq P_{\text{dis},p} \leq b_{\text{dis},p} P_{\text{BESS,max}} \quad (9)$$

$$b_{\text{ch},p} + b_{\text{dis},p} = 1 \quad (10)$$

and s.t. $\forall t \in \mathcal{T}$:

$$E_{\min} \leq E_t \leq E_{\max} \quad (11)$$

and s.t.:

$$E_0 = E_{\text{start}} \quad (12)$$

$$E_{24} = E_{\text{end}} \quad (13)$$

with:

$$E, P_{\text{ch},\text{dis}}, \hat{P}_{\text{grid},p} \in \mathbb{R} \quad (14)$$

$$b_{\text{ch}}, b_{\text{dis}} \in \{0, 1\} \quad (15)$$

EEq. (3) defines the objective function minimizing the daily electrical energy costs. Eq. (4) defines a set of indices for all time periods and Eq. (5) defines a set of indices for all time points. The power balance of the EC is defined in Eq. (6). Eqs. (7-11) describe the BESS model, where, η_{ch} and η_{dis} are the charging and discharging efficiencies, respectively and E_{\min} and E_{\max} denote minimum and maximum BESS capacity, respectively. The energy balance of the BESS is described in Eq. (7). Eqs. (8-10) prevent simultaneous charging and discharging via the binary variables b_{ch} and b_{dis} . The initial and the end conditions of the BESS are defined by Eqs. (12,13). The optimization uses the forecasted load P_{load} without a feedback loop, as real-time measurements over 50 households can be considered very difficult in practice. Consequently,

the grid is used to compensate forecast errors. The real, resulting grid power P_{grid} can therefore be described as such:

$$P_{\text{grid}} = P_{\text{ch}} - P_{\text{dis}} + P_{\text{load}} \quad (16)$$

where P_{load} is the real load of the EC. Consumption/energy from the power grid is priced via the RTP, while excess is fed into the grid without payment.

In the case study, a non-optimized reference case without utilization of the BESS is used as reference. Then, the different predictors for \hat{P}_{load} from Section 2 (using baseline configuration and one sample EC) are compared with a perfect prediction that assumes perfect knowledge of the future load. The optimization results of this case study are shown in Table 1.

Table 1: Case study optimization results for different prediction models.

Scenario	Costs (€)	Savings (€)	Reduction (%)
Reference	12787.91	-	-
Perfect	11345.03	1442.89	11.28
Synthetic	11632.05	1155.86	9.04
KNN	11612.99	1174.93	9.19
Persistence	11645.09	1142.83	8.94
xLSTM	11515.53	1272.39	9.95
LSTM	11517.03	1270.89	9.94
Transformer	11484.07	1303.85	10.20

Besides perfect prediction, which assumes perfect knowledge of the signal, the best results are achieved using the Transformer leading to savings of 1303.85€, which is equal to a cost reduction of 10.20%. LSTM and xLSTM perform nearly as well as Transformer with a cost reduction of 9.94% for LSTM and 9.95% for xLSTM. This shows that all three deep learning algorithms perform well and achieve savings of up to 161.02€ compared with persistent prediction over the investigated three months. For one year, these savings would scale to approximately 600€. In this case study, all prediction methods perform relatively well, because for RTP-driven load shifting, the price signal is the most important factor which is published one day in advance by EXAA. In contrast, other objectives, such as increasing self-sufficiency or reducing peak load are more prediction-sensitive, emphasizing the significance of high-quality predictions³⁰. This study demonstrates the suitability of deep learning for predicting electrical loads in an EC, with significant potential for load shifting to reduce operational costs.

5. Conclusions

This study provides insights into the performance of state-of-the-art forecasting models, assessed across diverse ECs, varying levels of aggregation, and differing sizes of training datasets.

One of the main findings of this study is that persistence prediction performs best when an EC has only six or fewer months of training data. However, as more data become available, models achieve lower forecast errors.

Furthermore, transfer learning from synthetic (standard) load profiles is a simple and effective approach to reduce the mean forecast error when training data is limited (up to 6 months, according to the results). However, despite this improvement, the above findings indicate that persistence prediction remains the preferred choice for such scenarios with fewer training data due to an even lower forecast error.

Although Transformer models are considered state-of-the-art for short-term load forecasting, still LSTM models continue to be a competitive option for the applications at hand. In addition, the newly introduced xLSTM models achieve accuracy comparable to Transformer models, offering a viable alternative. Generally, all deep learning models perform similar with no deep learning model showing clear superiority over all aggregation levels.

A case study quantifies the financial implication of the improvement between deep learning models and persistence prediction. The difference in forecast error of approximately 1.1%pt to 600€ annual savings for an EC of 50 households with a battery storage.

The software framework used for systematic evaluation of forecast errors in diverse ECs is publicly available. Other researchers are encouraged to benchmark models using this framework.

CRedit authorship contribution statement

Lukas Moosbrugger: Writing – Original Draft, Visualization, Software, Methodology, Data curation, Formal analysis, Conceptualization. **Valentin Seiler:** Writing – Review & Editing, Visualization, Methodology, Conceptualization. **Philipp Wohlgenannt:** Writing – Review & Editing, Software, Methodology, Conceptualization. **Sebastian Hegenbart:** Writing - Review & Editing, Methodology, Conceptualization. **Sashko Ristov:** Writing - Review & Editing, Methodology, Conceptualization. **Peter Kepplinger:** Writing – Review & Editing, Conceptualization, Supervision, Resources, Project administration, Funding acquisition.

Declaration of competing interest

The authors declare that they have no known competing financial interests or personal relationships that could have appeared to influence the work reported in this paper.

Data availability

This paper was created with a strong focus on transparency. Therefore, the data of the prediction method (including smartmeter load, weather, synthetic loads for pretraining, holiday calendar, etc.) are publicly accessible.

Only the EXAA price signal referenced in the case study section cannot be provided due to legal restrictions. However, users are encouraged to obtain this data independently, as it is freely available for download.

Acknowledgements

The authors gratefully acknowledge the financial support from the Austrian Research Promotion Agency FFG for the Hub4FIECs project (COIN FFG 898053).

Appendix A. Model Configuration

Table A.2 lists all the configurations of the deep learning models considered.

Appendix B. Extended Results

Tables B.3 and B.4 show additional results, including those for the KNN and Synthetic Load Profile benchmark predictors. These predictors were not included in the earlier figures because their errors were significantly higher compared to other predictors, which would have negatively impacted the clarity and readability of the visualizations.

Table A.2: Configuration of the xLSTM, LSTM, and Transformer of all model sizes (i.e. 1k, 2k, 5k, 10k, 20k, 40k, and 80k).

	Model Size	xLSTM	LSTM	Transformer
Input	Input Shape = (Batch_size, 24 hours, 20 features)			
Projection		Yes	No	Yes
Sequence Model	1k	Blocks = 1 Heads = 2 Features = 4 sLSTM at 0	Layer 1 = 1 Bi-LSTM Layer 2 = 1 Bi-LSTM	Layers = 1 Heads = 2 dim_feedforward = 10 Features = 10
	2k	Blocks = 1 Heads = 4 Features = 8 sLSTM at 0	Layer 1 = 4 Bi-LSTM Layer 2 = 4 Bi-LSTM	Layers = 1 Heads = 2 dim_feedforward = 10 Features = 16
	5k	Blocks = 2 Heads = 4 Features = 8 sLSTM at 1	Layer 1 = 8 Bi-LSTM Layer 2 = 9 Bi-LSTM	Layers = 1 Heads = 2 dim_feedforward = 10 Features = 90
	10k	Blocks = 2 Heads = 4 Features = 16 sLSTM at 1	Layer 1 = 10 Bi-LSTM Layer 2 = 18 Bi-LSTM	Layers = 1 Heads = 4 dim_feedforward = 10 Features = 200
	20k	Blocks = 2 Heads = 4 Features = 32 sLSTM at 1	Layer 1 = 22 Bi-LSTM Layer 2 = 1 Bi-LSTM	Layers = 1 Heads = 4 dim_feedforward = 10 Features = 400
	40k	Blocks = 4 Heads = 4 Features = 32 sLSTM at 1	Layer 1 = 42 Bi-LSTM Layer 2 = 1 Bi-LSTM	Layers = 1 Heads = 4 dim_feedforward = 10 Features = 400
	80k	Blocks = 4 Heads = 8 Features = 40 sLSTM at 1	Layer 1 = 70 Bi-LSTM Layer 2 = 21 Bi-LSTM	Layers = 2 Heads = 8 dim_feedforward = 400 Features = 40
Dense Layer 1	30 neurons, ReLU activation			
Dense Layer 2	20 neurons, ReLU activation			
Linear Layer	1 neuron, no activation			
Output	Output Shape = (Batch_size, 24 hours, 1 power value)			

Table B.3: Model comparison across different dimensions using the **mean nMAE (%) of 20 load profiles/models** and in brackets **standard deviation (%)** of these 20 load profiles/models. All models in this table were using transfer learning from synthetic load profiles. Every dimension started with the baseline, which means a training size of 12 month, 50 households aggregated, were tested on the last three month of 2013, and had $\sim 5k$ model parameters.

	Setup	Synth- etic	KNN	Persist- ence	xLSTM	LSTM	Trans- former
Model	1k	22.31	14.57	12.79	10.84	11.53	11.08
		(1.63)	(1.25)	(1.13)	(1.02)	(1.07)	(0.89)
Size	2k	22.31	14.57	12.79	10.91	10.81	11.17
		(1.63)	(1.25)	(1.13)	(1.04)	(0.92)	(0.89)
	5k	22.31	14.57	12.79	11.05	10.83	11.03
		(1.63)	(1.25)	(1.13)	(0.93)	(0.96)	(0.86)
	10k	22.31	14.57	12.79	11.71	10.88	11.05
		(1.63)	(1.25)	(1.13)	(0.97)	(0.87)	(0.89)
	20k	22.31	14.57	12.79	12.17	11.48	10.96
		(1.63)	(1.25)	(1.13)	(1.01)	(1.03)	(0.83)
40k	22.31	14.57	12.79	12.48	11.96	11.06	
	(1.63)	(1.25)	(1.13)	(1.08)	(0.96)	(0.82)	
80k	22.31	14.57	12.79	12.45	12.33	11.30	
	(1.63)	(1.25)	(1.13)	(0.98)	(1.10)	(1.01)	
Testset (2013)	Q1	23.19	14.85	12.79	11.89	11.52	11.82
		(1.74)	(1.13)	(1.13)	(1.61)	(1.22)	(1.37)
	Q2	38.13	14.60	11.89	10.66	10.48	10.14
		(5.51)	(1.39)	(0.97)	(0.80)	(0.78)	(0.87)
	Q3	28.45	17.60	14.54	12.56	12.19	12.16
	(3.54)	(1.44)	(1.01)	(1.17)	(1.16)	(1.13)	
	Q4	29.09	16.32	14.02	11.87	12.78	12.16
		(3.27)	(2.01)	(1.64)	(1.56)	(1.59)	(1.54)
Community Size	1	100.45	68.44	57.25	49.66	49.95	50.56
		(41.53)	(18.69)	(17.94)	(12.33)	(12.23)	(15.04)
	2	67.25	49.40	44.98	37.41	36.78	37.21
		(44.36)	(16.30)	(17.17)	(10.47)	(9.33)	(9.57)
	10	34.96	28.50	24.86	21.10	20.83	21.41
		(5.96)	(4.10)	(3.13)	(2.96)	(3.01)	(3.29)
	50	22.31	14.57	12.79	11.05	10.83	11.03
		(1.63)	(1.25)	(1.13)	(0.93)	(0.96)	(0.86)
	100	20.96	11.36	10.10	8.55	8.31	8.53
		(1.14)	(0.77)	(0.49)	(0.38)	(0.40)	(0.49)
Training Size	2 mo	28.86	20.03	12.79	14.94	15.00	16.55
		(2.67)	(2.11)	(1.13)	(2.10)	(1.86)	(3.28)
	4 mo	29.43	20.12	12.79	13.92	15.32	15.68
		(2.84)	(2.14)	(1.13)	(1.22)	(1.67)	(2.50)
	6 mo	27.09	19.01	12.79	13.44	14.32	14.28
		(2.54)	(1.84)	(1.13)	(1.35)	(1.90)	(2.06)
	9 mo	23.19	14.85	12.79	11.89	11.52	11.82
		(1.74)	(1.13)	(1.13)	(1.61)	(1.22)	(1.37)
	12 mo	22.31	14.57	12.79	11.05	10.83	11.03
		(1.63)	(1.25)	(1.13)	(0.93)	(0.96)	(0.86)
	15 mo	23.06	14.64	12.79	11.07	10.80	11.04
		(1.77)	(1.21)	(1.13)	(0.91)	(0.89)	(0.84)

Table B.4: Model comparison **without transfer learning** across different dimensions using the **mean nMAE (%) of 20 load profiles/models** and in brackets the **standard deviation (%)**.

	Setup	Synth- etic	KNN	Persist- ence	xLSTM	LSTM	Trans- former
Training	2 mo	28.86 (2.67)	20.03 (2.11)	12.79 (1.13)	16.58 (2.63)	17.53 (2.95)	18.47 (3.97)
Size	4 mo	29.43 (2.84)	20.12 (2.14)	12.79 (1.13)	16.21 (1.64)	16.33 (2.07)	16.03 (2.34)
	6 mo	27.09 (2.54)	19.01 (1.84)	12.79 (1.13)	14.39 (2.31)	14.44 (1.56)	14.96 (2.34)
	9 mo	23.19 (1.74)	14.85 (1.13)	12.79 (1.13)	12.03 (1.34)	11.43 (1.07)	12.04 (1.59)
	12 mo	22.31 (1.63)	14.57 (1.25)	12.79 (1.13)	11.18 (1.00)	10.82 (0.87)	11.13 (0.90)
	15 mo	23.06 (1.77)	14.64 (1.21)	12.79 (1.13)	11.11 (0.97)	10.83 (0.88)	11.12 (0.79)

References

- [1] D. Mariano-Hernández, L. Hernández-Callejo, A. Zorita-Lamadrid, O. Duque-Pérez, F. S. García, A review of strategies for building energy management system: Model predictive control, demand side management, optimization, and fault detect & diagnosis, *Journal of Building Engineering* 33 (2021) 101692. doi:10.1016/j.jobee.2020.101692.
- [2] C. Srithapon, D. Månsson, Predictive control and coordination for energy community flexibility with electric vehicles, heat pumps and thermal energy storage, *Applied Energy* 347 (2023) 121500. doi:10.1016/j.apenergy.2023.121500.
- [3] R. Wazirali, E. Yaghoubi, M. S. S. Abujazar, R. Ahmad, A. H. Vakil, State-of-the-art review on energy and load forecasting in microgrids using artificial neural networks, machine learning, and deep learning techniques, *Electric power systems research* 225 (2023) 109792. doi:10.1016/j.epsr.2023.109792.
- [4] European Commission, Clean energy for all Europeans, Publications Office of the European Union, 2019. doi:10.2833/9937.
- [5] S. Van Der Stelt, T. AlSkaif, W. Van Sark, Techno-economic analysis of household and community energy storage for residential prosumers with

- smart appliances, *Applied Energy* 209 (2018) 266–276. doi:10.1016/j.apenergy.2017.10.096.
- [6] W. Kong, Z. Y. Dong, Y. Jia, D. J. Hill, Y. Xu, Y. Zhang, Short-term residential load forecasting based on LSTM recurrent neural network, *IEEE Transactions on Smart Grid* 10 (1) (2019) 841–851. doi:10.1109/TSG.2017.2753802.
- [7] F. Pallonetto, C. Jin, E. Mangina, Forecast electricity demand in commercial building with machine learning models to enable demand response programs, *Energy and AI* 7 (2022) 100121. doi:10.1016/j.egyai.2021.100121.
- [8] L. Semmelmann, M. Hertel, K. J. Kircher, R. Mikut, V. Hagemeyer, C. Weinhardt, The impact of heat pumps on day-ahead energy community load forecasting, *Applied Energy* 368 (2024) 123364. doi:10.1016/j.apenergy.2024.123364.
- [9] P. Ran, K. Dong, X. Liu, J. Wang, Short-term load forecasting based on ceemdan and transformer, *Electric Power Systems Research* 214 (2023) 108885. doi:10.1016/j.epsr.2022.108885.
- [10] Z. Zhao, C. Xia, L. Chi, X. Chang, W. Li, T. Yang, A. Y. Zomaya, Short-term load forecasting based on the transformer model, *information* 12 (12) (2021) 516. doi:10.3390/info12120516.
- [11] A. L’Heureux, K. Grolinger, M. A. Capretz, Transformer-based model for electrical load forecasting, *Energies* 15 (14) (2022) 4993. doi:10.3390/en15144993.
- [12] B. Fang, L. Xu, Y. Luo, Z. Luo, W. Li, A method for short-term electric load forecasting based on the fmlp-itransformer model, *Energy Reports* 12 (2024) 3405–3411. doi:10.1016/j.egyr.2024.09.023.
- [13] M. Beck, K. Pöppel, M. Spanring, A. Auer, O. Prudnikova, M. Kopp, G. Klambauer, J. Brandstetter, S. Hochreiter, xLSTM: Extended Long Short-Term Memory, in: *Thirty-eighth Conference on Neural Information Processing Systems*, 2024. doi:10.48550/arXiv.2405.04517.

- [14] M. Kraus, F. Divo, D. S. Dhimi, K. Kersting, xlstm-mixer: Multivariate time series forecasting by mixing via scalar memories, arXiv preprint (2024). doi:10.48550/arXiv.2410.16928.
- [15] E. Lee, W. Rhee, Individualized short-term electric load forecasting with deep neural network based transfer learning and meta learning, IEEE Access 9 (2021) 15413–15425. doi:10.1109/ACCESS.2021.3053317.
- [16] M. Ribeiro, K. Grolinger, H. F. ElYamany, W. A. Higashino, M. A. Capretz, Transfer learning with seasonal and trend adjustment for cross-building energy forecasting, Energy and Buildings 165 (2018) 352–363. doi:10.1016/j.enbuild.2018.01.034.
- [17] L. Moosbrugger, V. Seiler, G. Huber, P. Kepplinger, Improve load forecasting in energy communities through transfer learning using open-access synthetic profiles, in: 2024 IEEE 8th Forum on Research and Technologies for Society and Industry Innovation (RTSI), IEEE, 2024, pp. 31–35. doi:10.48550/arXiv.2407.08434.
- [18] M. G. Pinheiro, S. C. Madeira, A. P. Francisco, Short-term electricity load forecasting—a systematic approach from system level to secondary substations, Applied Energy 332 (2023) 120493. doi:10.1016/j.apenergy.2022.120493.
- [19] Energy Research Centre, Vorarlberg University of Applied Sciences, Github repository for load forecasting, <https://github.com/rce-fhv/loadforecasting/>, accessed: 2024-12-10 (2024).
- [20] Austrian Coordination Office for Energy Communities, Energy communities map, <https://energiegemeinschaften.gv.at/landkarte/>, accessed: 2024-12-10 (2024).
- [21] A. Groß, A. Lenders, F. Schwenker, D. A. Braun, D. Fischer, Comparison of short-term electrical load forecasting methods for different building types, Energy Informatics 4 (Suppl 3) (2021) 13. doi:10.1186/s42162-021-00172-6.
- [22] Y. Nie, N. H. Nguyen, P. Sinthong, J. Kalagnanam, A time series is worth 64 words: Long-term forecasting with transformers, in: The Eleventh International Conference on Learning Representations, 2023.

doi:10.48550/arXiv.2211.14730.

URL <https://openreview.net/forum?id=Jbdc0vT0col>

- [23] D. P. Kingma, J. Ba, Adam: A method for stochastic optimization, in: 3rd International Conference on Learning Representations, ICLR 2015, San Diego, CA, USA, May 7-9, 2015, Conference Track Proceedings, 2015. doi:10.48550/arXiv.1412.6980.
- [24] C. S. Lamprecht, Meteostat Python, accessed on 11 December 2024.
URL <https://github.com/meteostat/meteostat-python>
- [25] G. Van Rossum, F. L. Drake, Python 3 Reference Manual, CreateSpace, Scotts Valley, CA, 2009.
- [26] J. Ansel, E. Yang, H. He, N. Gimelshein, A. Jain, M. e. a. Voznesensky, PyTorch 2: Faster Machine Learning Through Dynamic Python Bytecode Transformation and Graph Compilation, in: 29th ACM International Conference on Architectural Support for Programming Languages and Operating Systems, Volume 2 (ASPLOS '24), ACM, 2024. doi:10.1145/3620665.3640366.
URL <https://pytorch.org/assets/pytorch2-2.pdf>
- [27] EPEX SPOT, accessed on 11 December 2024.
URL <https://www.epexspot.com/en>
- [28] EXAA - Die Strombörse mit fünf Auktionen in AT, DE und NL, accessed on 11 December 2024.
URL <https://www.exaa.at/>
- [29] W. Cole, A. W. Frazier, C. Augustine, Cost Projections for Utility-Scale Battery Storage: 2021 Update, Tech. Rep. NREL/TP-6A20-79236, National Renewable Energy Lab. (NREL), Golden, CO (United States) (2021). doi:10.2172/1786976.
- [30] P. Wohlgenannt, G. Huber, K. Rheinberger, M. Kolhe, P. Kepplinger, Comparison of demand response strategies using active and passive thermal energy storage in a food processing plant, Energy Reports 12 (2024) 226–236. doi:<https://doi.org/10.1016/j.egyrs.2024.06.022>.